https://erjm.journals.ekb.eg
ISSN: 1110-1180

DOI: 10.21608/erjm.2021.36627.1033

ERJ
Engineering Research Journal
Faculty of Engineering
Menoufia University

Experimental and Numerical Analysis of Steel Beam-Column Connections

Mohamed E. Nawar[1*], Ahmed A. Elshafy[2], Boushra A. Eltaly[2], Kamel S. Kandil[2]

[1] *PhD Candidate, Department of Civil Eng., Faculty of Eng., Menoufia University, Egypt.*
[*]*Department of Civil Eng., Higher Institute of Engineering and Technology, Kafr Elsheikh, Egypt.*
[2]*Department of Civil Eng., Faculty of Eng., Menoufia University, Egypt.*

Abstract
This paper presents experimentally and numerically the analysis of beam to column steel connections in extended end plate form. The study aims to calibrate a finite element model (FEM) able to predict these connections with high accuracy. Tests of two specimens of the beam to column end plate connections under monotonic load up to failure were presented. The tested connections were analyzed numerically using proposed (FEM) using ANSYS software that included nonlinearities of material, contact, and geometric. The study compared the test and FEM results through discussion of applied load versus vertical deflection and the deformed shape of the end plate and the bolts that consider the main component of the connection. Also, the moment rotation (M-θ) curve was plotted and discussed. The characteristics of the M-θ curve of each connection were determined and compared with its Eurocode 3 counterparts. The comparison revealed a good agreement between the results. The effect of end plate thickness on the characteristics of M-θ curve was presented.

Keywords: *End plate connections; Moment rotation curve; Finite Element Analysis; ANSYS; Beam–Column Steel Connection.*

1. Introduction

Bolted end plate connections are considered as one of the most common beams to column connections in recent years; in particularly extended end plate connection. End plate connections comprise a plate which is welded to the beam end and connected to the column flange using bolts. They have many advantages such as their economy, simplicity of fabrication, good structural performance; especially under dynamic loads [1-4]. Moment rotation (*M-θ*) is considered as the significant tool that can be used to represent the behavior of the beam to column connections. Several methods are used to get this relationship such as experimental testes, analytical analysis, and numerical analysis. With the tremendous development in the computer and structural analysis programs, designers have been able to obtain the behavior of structural elements with high accuracy, as well as saving great effort and cost of laboratory tests. Nowadays, commercial programs such as ANSYS and ABAQUS have many elements and material libraries for the solution of nonlinear material and geometric problems in structural mechanics. Recently, many researchers rely on calibrating a finite element model (FEM) based on the comparison of the results with the previous experimental results to complete their researches.

Díaz C. et al. [3] used the experimental model carried out by Janss *et al.* [5] to verify a 3D FEM using ANSYS software program to obtain the behavior of steel end plate beam-to-column connections. Bai *et al.* [6] verified a FEM based on seven extended end plate connections tested by Shi Gang [7] to study the improvement design of extended end plate joints that have prying force effects. Chen *et al.* [8] used the numerical analysis by the finite element analysis software ABAQUS, based on the two experimental specimens were tested, to study the effect of end plate stiffened on the initial rotational stiffness of extended end plate of internal joints. Dessouki *et al.* [20] conducted a parametric study on end plate connections in two configurations; four bolts and multiple rows extended end plates using a calibrated FEM with the experimental work of Sumner [9]. Salem *et al.* [10, 11] developed a FEM and calibrated it against the experimental results to carry a parametric study to investigate the end plate in both configurations; extended end plate and flush end plate. Louis and Babu [12] used ANSYS Workbench 16.1 software to study numerically the behavior of bolted steel beam to column end plate connections due to strengthening. Samaan *et al.* [13] used a FEM calibrated with their experimental work in the same study in addition to experimental results recorded by other researchers to study the large capacity of extended end plate connections. Zeinoddini-Meimand *et al.* [14] used the finite element analysis to study effect of cyclic load on flush end plate connection.

2. Aim and Research Significance

This paper presents the experimental and numerical analysis of steel beam-column bolted end plate connections. This study aims to calibrate a FEM able to predict these connections with high accuracy. Two specimens of the beam to column end plate connections were tested experimentally and analyzed numerically

using ANSYS software. Nonlinearities of material, FEM. The results of the two approaches of the analysis were compared in terms of moment rotation curve (*M-θ*), point load displacement, and deformed shape. Also, the characteristics of the *M-θ* curve for two connections were derived and compared with the prediction of Eurocode 3 [19].

3. Experimental Program

The experimental work contains two specimens of the full scale of the cantilever beam to column connections in the extended end plate form as shown in Fig. 1. The cantilever beam was comprised from the standard HEB 200 with length 750 *mm*. The cantilever has been reinforced with haunch as a part from the same section of the beam as presented in Fig. 1. The haunch was added to prevent any weld failure occurrence. The column comprised from three plates with length 1000 *mm*. Two plates were used for flanges with 200 × 300 *mm* cross section and one plate with 240 × 200 *mm* for web section. The cantilever and column were stiffened at the concentrated stress regions as shown in Fig. 1. The two end plates have 200 × 440 *m*m dimensions with 12 *mm* and 15 *mm* thickness. All plates and parts were assembled using welding process. End plates were welded to the cantilevers and connected to the column flange with six bolts arranged. All bolts have 20 *mm* nominal diameter and grade 8.8. The specimen's components were designed so that the failure is limited to the bolts and/or end plate without the development of any plastic moment in cantilever beam or weld. The column plates were designed to behave as a rigid behavior. Each specimen has name contains three parts; C, bolts diameter, and end plate thickness, i.e. the first and the second specimens have names C-20-12 and C-20-15, respectively.

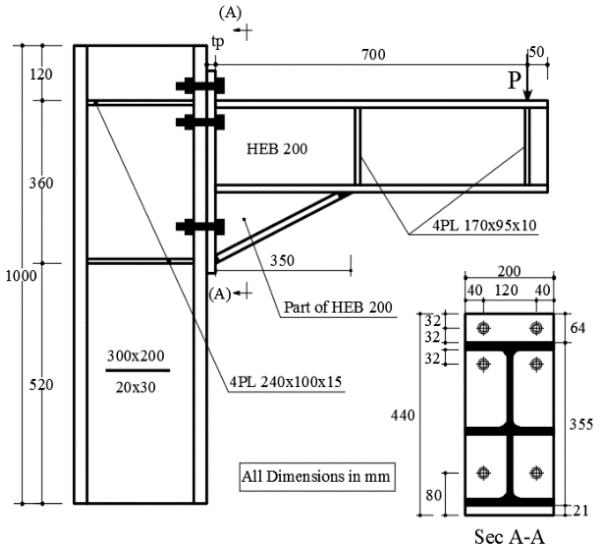

Fig. 1- Details of Specimens.

For each specimen, the displacements of the end plates were measured in eight different locations and the vertical displacement of point load using measurements devices Pi-Gauges and Linear Variable Displacement Transducer. Herein, the study focused on the two contact, and geometric were included in the proposed measurements of the end plate deformation needed to calculate the connections rotations and the vertical displacement at the point load to calibrate the proposed numerical model. The gap between the end plate and column flange at the top beam flange level was measured by two Pi-Gauges and the vertical displacement at point load was measured by Linear Variable Displacement Transducer (LV).

Fig. 2 shows the distribution of instrumentations. A permanent load of 500 kN was applied on the column top with 100 *mm* eccentricity to reduce the generated bending moment on the column base. Then, the test was started after the recorded readings were zeroed followed by applied monotonic load up to the failure of specimen.

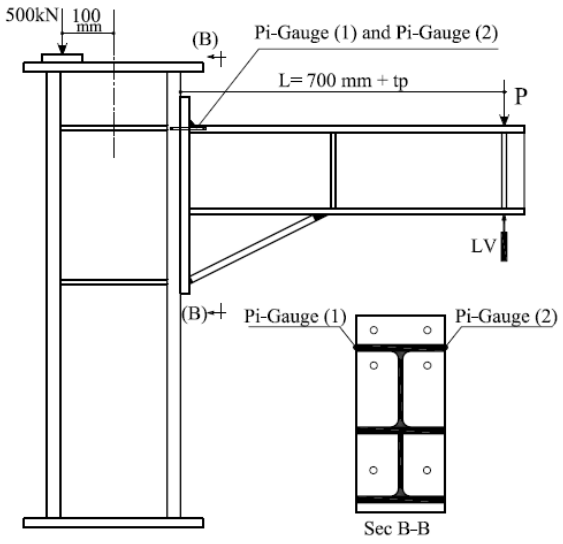

Fig. 2- Instrumentations Distribution.

4. Finite Element Model

The finite element program, ANSYS workbench was used to simulate the tested connections numerically. The numerical models were built according to Fig. 1 using the commercial software package, Solidworks then imported to ANSYS Workbench. All connections components were modeled using 8-nodes solid structural element SOLID185. SOLID185 element is suitable for modeling of 3D solid structures in two forms: homogeneous and layered structure. It is defined by 8-nodes, each node has three degrees of freedom (translation in three global axes directions). The element allows defining plasticity, hyperelasticity, stress stiffening, creep, large deflection, and large strain capabilities [18]. Surface-to-surface contact elements CONTA173 and TARGE170 were used to define the contact between the adjacent parts. Bonded contact was imposed between all adjacent parts except between end plate and column flange, bolts head and washers, and holes and bolts' shanks. The contact between the column flange and end plate is friction contact with coefficient 0.2 and also for the contact between bolts head and washers. Due to existing clearance in bolts holes, the

contact between bolts' shanks and holes was provided as frictionless contact. The material properties for each component of the connections were defined according to the coupon tensile test as showed in Table 1. Poisson's ratio was taken as 0.3. The Multilinear kinematic hardening was used to represent the nonlinear stage of stress strain curve. The column base was defined as fixed support in addition to a permanent load 500 kN was defined on the column top as shown in Fig. 3. The recorded applied load during the experimental test were defined to the FEM and the corresponded locations of two Pi-Gauges and LV were determined.

Table 1- Mechanical Properties of the Connection Components.

Element Part		(f_y) (MPa)	(f_u) (MPa)	(E) (MPa)	ε_u	ε_f
Column Plate (Average)	web / flange	250.51	429.61	194,449	0.179	0.236
Beam (Average)	web / flange	291.90	439.20	184,650	0.109	0.148
Plates	t = 10 mm	244.17	396.00	181,180	0.13	0.185
	t = 12 mm	339.09	492.00	181,260	0.103	0.12
	t = 15 mm	352.28	502.72	205,536	0.138	0.192
Bolts	D = 20 mm	811.11	942.00	210,000		

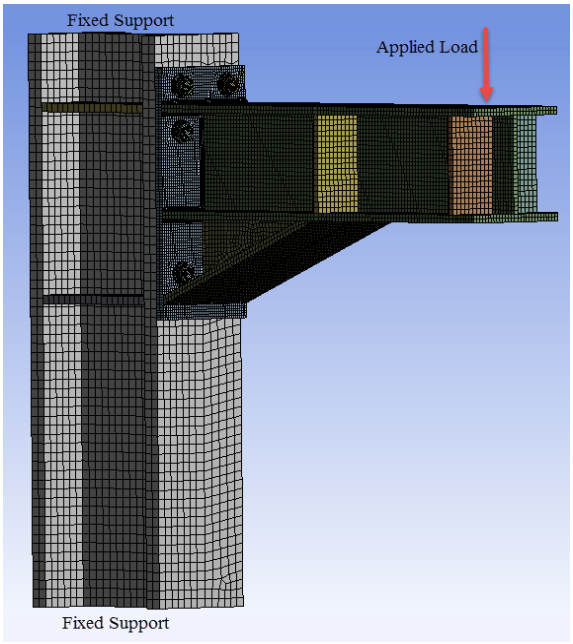

Fig. 3- Finite Element Model.

5. Results Discussion and Validation

5.1. Specimens Deformation

Figs. 4 and 5 show a comparison between the deformed shape of the two studied connections due to the experimental test and the proposal FEM. The comparison indicates to the validity of the FEM to predict the behavior of these connections. For specimen C-20-12, the deformed shape of the connection started with form a gap between the end plate and the column flange in the level of beam upper flange. At the end, the end plate in the upper zone was bent and the upper for bolts were elongated followed by bending. In addition to, an extension of the gap up to the level of lower beam flange is occurred. For specimen C-20-15, the separation between the end plate and the column flange in the region between the upper four bolts accompanied by its elongation was observed at the loading beginning. Then the separation extended gradually up to the level of the cantilever bottom flange.

Also, the separation extended up to the upper edge of the end plate. The maximum gap was observed at the upper welded edged of the end plate. Shortly before the end, a slight bending of the upper two bolts occurred. The relationship between the point load and deflection for both test and FEM results was shown in Figs. 6 and 7.

The load-deflection curves show that FEM agrees with the test results with a slight discrepancy in the linear stage slope does not exceed 5%. As for the nonlinear stage, there is a bit different in maximum applied load 10% at most.

a) Test

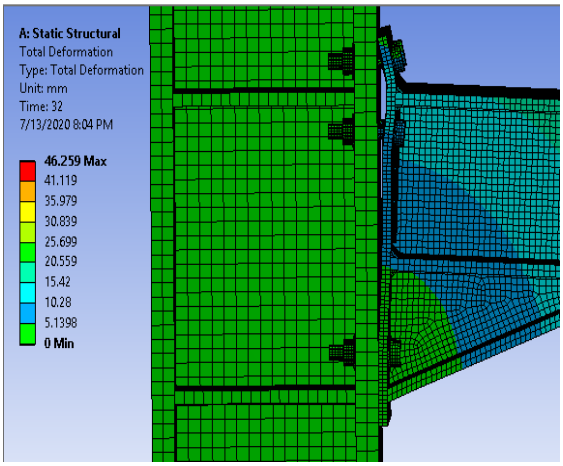

b) FEM

Fig. 4- Deformed Shape of Connection C-20-12.

a) Test.

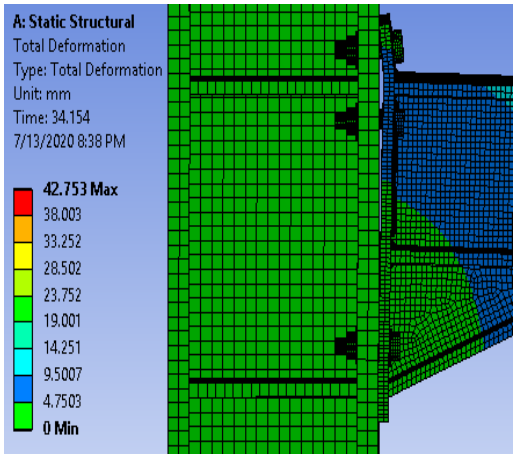

b) FEM.

Fig. 5- Deformed Shape of Connection C-20-15.

5.2. Moment-Rotation Relationship

The acting moment on the connection M was taken as the product of applied load multiplied by the moment arm (L = 700 mm + thickness of end plate (t_p)) as illustrated in Eq. 1 and Fig. 2.

Rotation of the connections (θ) was determined by dividing the average recorded readings of two Pi-Gauges by the lever arm (z) [15, 16] as illustrated in Eq. 2 and Fig. 8. Lever arm (z) is the distance between mid of the upper and the bottom beam flange. M-θ curves were plotted for the two connections according to Eq. 1 and 2.

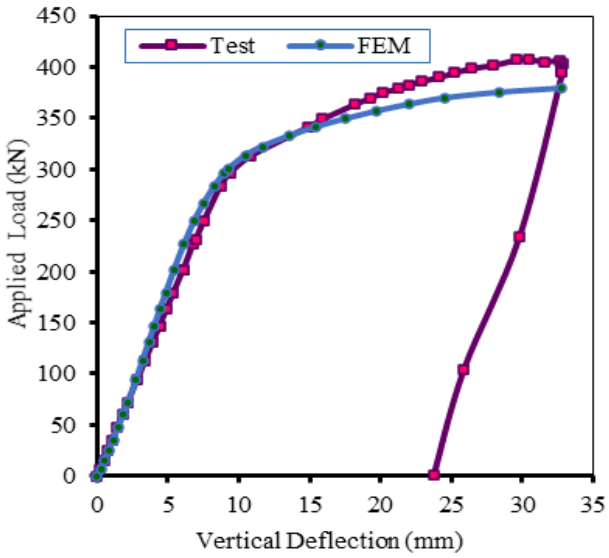

Fig. 6- Applied Load versus Vertical Displacement Relationship of Specimen C-20-12.

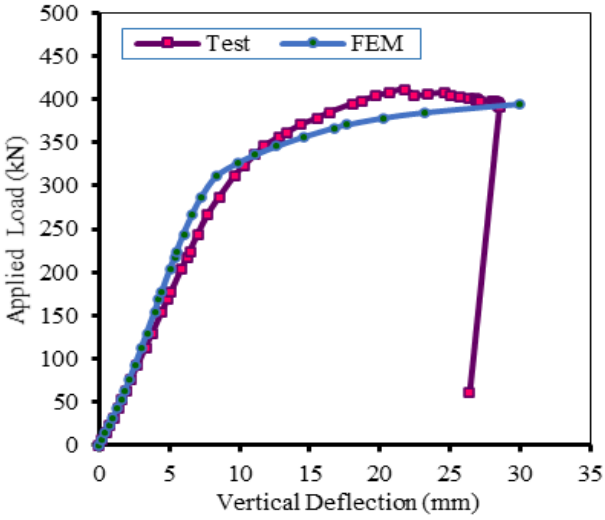

Fig. 7- Applied Load versus Vertical Displacement Relationship of Specimen C-20-15.

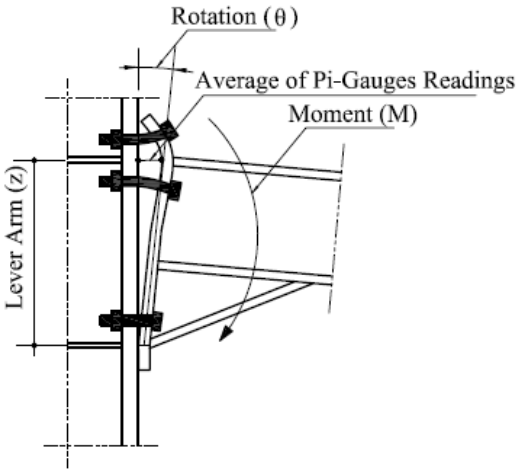

Fig. 8- Parameters of Moment Rotation Relationship.

$$M = P \times L \quad (1)$$

$$\theta = \arctan\left(\frac{Average\ of\ two\ Pi - Gauges\ reading}{z}\right)$$

Fig. 9 and Fig. 10 show *M-θ* curve for specimens C-20-12 and C-20-15 due to the experimental test and the proposal FEM, respectively. From the two figures, there is a good agreement between the FEM and the test results with a slight discrepancy in the slope of the linear stage of specimen C-20-15 and nonlinear stage of specimen C-20-12. The characteristics of each *M-θ* curve due to the test and FEM were determined according to Coelho et al. [17] as illustrated in Fig. 11.

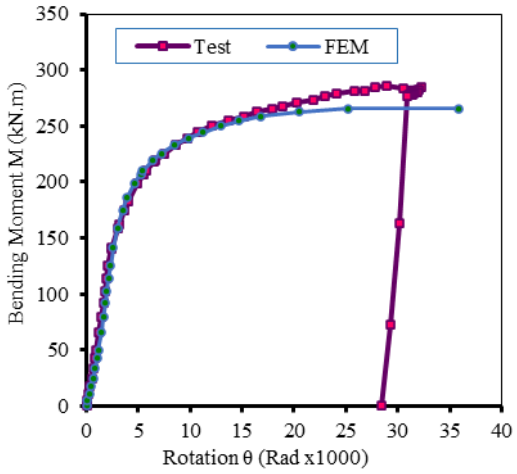

Fig. 9- Moment Rotation Relationship of Specimen C-20-12.

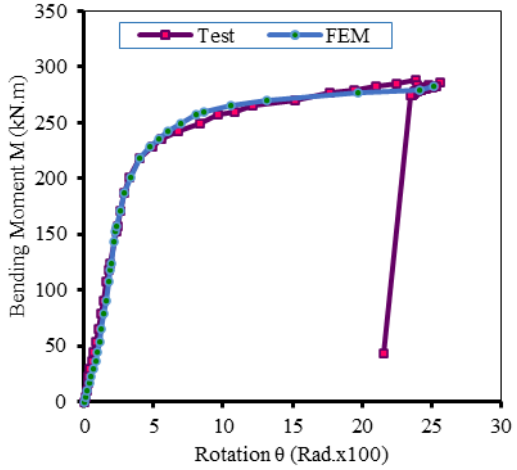

Fig. 10- Moment Rotation Relationship of Specimen C-20-15.

Also, the main characteristics according to the Eurocode 3; yield moment M_y, Plastic moment capacity M_{Rd}, and Rotational stiffness S_{in}, were determined (See Eq. 3, 4, and 5). Table 2 shows summary and comparison between the predication of *M-θ* curve characteristics due to test, FEM, and Eurocode 3 approach. Also, the table illustrates the definition of *M-θ* curve that showed in Fig. 11.

$$M_{Rd} = \sum_i h_i F_i \quad (3)$$

$$M_y = \frac{2}{3} M_{Rd} \quad (4)$$

$$S_{in} = \frac{E z^2}{\sum_n \frac{1}{k_n}} \quad (5)$$

Where: h_i is the distance from the bolt-row *i* to the center of the bottom flange, F_i is the effective design tension resistance of bolt-row *i*, E is the modulus of steel elasticity, z is the lever arm, and K_n is the stiffness coefficient for basic joint component n . For more details about these equations see Eurocode 3 (EN 1993-1-8:2005) chapter six [19].

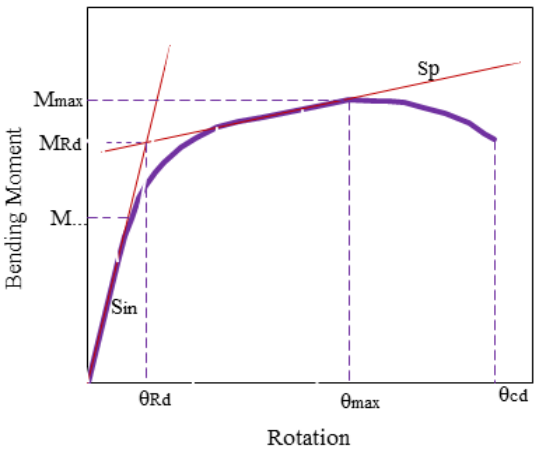

Fig. 11- Definition of Moment rotation curve characteristics according to Coelho et al. [17].

The comparison shown in Table 2 indicates that the proposed FEM and the experimental test are in perfect agreement to predict the initial rotational stiffness, the yield moment, and the plastic moment capacity with a difference does not exceed 8% in the initial rotational stiffness for specimen C-20-15. As for the Eurocode 3 prediction for the three characteristics, there is difference 6% and 2% for yield moment, 11% and 7.5% for the plastic moment capacity, and 10% and 5.5% for the initial rotational stiffness for both specimens C-20-12 and C-20-15; respectively. About the remaining five characteristics, the comparison was limited between the experimental test and the FEM because they are not including in Eurocode 3 [19]. The differences in these characteristics do not exceed 10% as shown in Table 2.

5.3. Effect of End Plate Thickness

From Figs. 9 and 10 and Table 2, the effect of the end plate thickness on the behavior of the studied connections can easily be deduced. By increasing the thickness of the end plate from 12 *mm* to 15 *mm*, the yield moment, the plastic moment capacity and the initial rotational stiffness increase by about 20%, 11% and 15%, respectively, as the average for the test, the FEM, and the Eurocode 3 predictions. As for the maximum moment capacity, it is not significantly affected where the increase does not exceed 1% for the test results and 6% for the FEM. While the effect was very clear in the decrease of the ductility at the increase of the end plate thickness because of the decrease of the final rotational. The rotation of the specimen C-20-15 at the failure was less than C-20-12 with 21% and 30% for the test and the FEM; respectively.

Table 2- Moment-Rotation Curve Characteristics.

Characteristic		Analysis method	C-20-12	C-20-15
Yield Moment M_y (kN.m)		Test	125.43	152.32
		FEM	124.20	150.27
		Eurocode	132.70	150.41
Plastic moment capacity M_{Rd} (kN.m)		Test	222.78	244.24
		FEM	221.55	248.56
		Eurocode	199.05	225.62
Rotational stiffness S_{in} (kN.m/rad)		Test	57535	66067
		FEM	57929	71332
		Eurocode	63571	69763
Maximum moment capacity M_{max} (kN.m)		Test	285.60	288.22
		FEM	265.61	282.74
Post –limit stiffness S_p (kN.m/rad)		Test	3216	2130
		FEM	3223	2212
Rotational capacities (rad x 1000)	θ_{Rd}	Test	7.20	7.30
		FEM	6.80	6.90
	θ_{max}	Test	28.99	23.86
		FEM	25.23	25.18
	θ_{cd}	Test	32.23	25.59
		FEM	35.81	25.18

6. CONCLUSIONS

This paper presents experimentally and numerically the analysis of beam to column steel connections in extended end plate form. The finite element model using the software ANSYS program was proposed. The proposed model included the nonlinearities of material, contact, and geometric. The study compared the test and FEM results through discussion of the deformed shape of the end plate and the bolts that consider the main component of the connection. Also, the moment rotation curve was plotted and discussed. The characteristics of the *M-θ* curve of each connection were determined according to Coelho et al. [17] and compared with its Eurocode 3 counterparts and additionally the present of the effect of end plate thickness on the connection behavior. From the previous discussions, the following conclusions were concluded:

- The proposal FEM gives good results in comparison to the test results or the Eurocode and it can be relied upon in similar future studies.
- The experimental and numerical results proved that the lower flange of the beam is the boundary between the separation and the connecting regions between the plate and the column flange, which is consistent with the assumptions of the Eurocode 3 [19].
- As the thickness of the end plate increases from 12 *mm* to 15 *mm*, with 20 *mm* bolts diameter, the loading capacity of the connection increases, but this is accompanied by a decrease in the connection ductility.

5. References

[1] A. S. Sherbourne and M. R. Bahaari, "3D Simulation of End-Plate Bolted Connections" Journal of Structural Engineering, 120 (11), 3122-3136, 1994.

[2] M. R. Mohamadi-Shoorea and M. Mofidb, "Basic Issues in the Analytical Simulation of Unstiened Extended End Plate Connection", Scientia Iranica, 11(4), 303-311, 2004.

[3] C. Díaz, M. Victoria, P. Martí, and O. M. Querin, "FE model of beam-to-column extended end-plate joints", Journal of Constructional Steel Research, 67, 1578–1590, 2011.

[4] R. E. S. Ismail, A.S. Fahmy, A. M. Khalifa, and Y. M. Mohamed, "Numerical Study on Ultimate Behavior of Bolted End-Plate Steel Connections" Latin American Journal of Solids and Structures, 13, 1-22, 2016.

[5] J. Janss, JP. Jaspart, and R. Maquooi. Experimental study of the non-linear behaviour of beam-to-column bolted joints. In: Reidar Bjorhovde, Jacques Brozzetti, AndréColson, editors. Connections in steel structures: behaviour, strength and design. Elsevier Ap-plied Science; 1987. p. 26–32.

[6] R. Bai, S. Chan, and J. Hao, "Improved design of extended end-plate connection allowing for prying effects", Journal of Construc-tional Steel Research, 113, 3–27, 2015.

[7] Shi Gang, Static and Seismic Behavior of Semirigid End-plate Connections in Steel Frames, Tsinghua University, Beijing, 2004.

[8] S. Chen, C. Chao Zhou and Z. Wang, "Experimental Study and Comparative Numerical Analysis of the Mechanical Behavior of Extended End-Plate Connections with End-Plate Stiffeners", The Open Mechanical Engineering Journal, 9, 653-665, 2015.

[9] EA. Sumner. Unified design of extended end-plate moment con-nections subject to cyclic loading. PhD thesis. Virginia Polytechnic Institute and State University, USA; 2003.

[10] A. H. Salem, E. Y. Sayed-Ahmed, A. A. El-Serwi, and R. A. Aziz, "Behavior and Design of I-Beam-To-Column Connections: Extended Rigid Bolted Connections", EUROSTEEL 2014, Naples, Italy, September 10-12, 2014.

[11] A. H. Salem, E. Y. Sayed-Ahmed, A. A. El-Serwi, and R. A. Aziz, "Behavior and Design of I-Beam-To-Column Connections: Flushed Rigid Bolted Connections", EUROSTEEL 2014, Naples, Italy, September 10-12, 2014.

[12] L. Louis and N. Babu, "Numerical Analysis of Strength Behavior of Bolted Steel Beam Column Connection Based on Type and Position of Stiffeners", International Research Journal of Engineering and Technology (IRJET), 4(4), 3205-3211, 2017.

[13] R. A. Samaan, A. I. El-Serwi, and R. A. El-Hadary, "Experimental and theoretical study of large capacity extended end-plate moment connection", EUROSTEEL 2017, Copenhagen, Denmark, September 13–15, 2017.

[14] V. Zeinoddini-Meimand, M. Ghassemieh, and J. Kiani, "Finite Element Analysis of Flush End Plate Moment Connections under Cyclic Loading" International Journal of Civil and Environmental Engineering, 8(1), 96-104, 2014.

[15] G. Shi, YJ. Shi and YQ. Wang "Behavior of end-plate moment connections under earthquake loading". Engineering Structures, 29(5), 29(5):703–716, 2007.

[16] G. Shi, Y. Shi, Y. Wang, and F. S. K. Bijlaard, "Monotonic loading tests on semi-rigid end-plate connections with welded I-shaped columns and beams", Advances in Structural Engineering, 13(2), 215-230, 2010.

[17] A. Coelho, F. Bijlaard, and L. Silva, "Experimental assessment of the ductility of extended end plate connections", Engineering Structures, 26, 1185-1206, 2004.

[18] ANSYS Workbench Help, Version 19.

[19] European Committee for Standardization (CEN). Eurocode 3. Design of steel structures, Part 1–8: design of joints (EN 1993-1-8:2005), 2005. Brussels.

[20] D. Abdelrahim, Y. Ahmed and I. Mohamed, "Behavior of I-beam bolted extended end-plate moment connections", Ain Shams Engineering Journal, 4, 685–699, 2013.